Frontiers in Bioscience Landmark

Front. Biosci. (Landmark Ed) **2026**; 31(2): 46251
https://doi.org/10.31083/FBL46251

Original Research

LXN-THBS2 Signaling Axis Regulates Hepatic Stellate Cell Activation and Promotes the Development of Liver Fibrosis

Haoyan Wang[1,2,†], Hanyu Jiang[1,3,†], Suyi Wang[1,3], Xinru Luo[1,2], Xi Tan[1], Donglin Cao[1,3,4], Yachao Yao[1,3,4,*]

[1]Department of Laboratory Medicine, The Affiliated Guangdong Second Provincial General Hospital of Jinan University, 510317 Guangzhou, Guangdong, China
[2]The Fourth Clinical Medical College, Jinan University, 510317 Guangzhou, Guangdong, China
[3]The Second Clinical Medical College, Guangdong Medical University, 510317 Guangzhou, Guangdong, China
[4]The Second School of Clinical Medicine, Southern Medical University, 510317 Guangzhou, Guangdong, China
*Correspondence: yaoych@gd2h.org.cn (Yachao Yao)
[†]These authors contributed equally.
Academic Editor: Vesna Jacevic
Submitted: 2 September 2025 Revised: 3 December 2025 Accepted: 16 December 2025 Published: 6 February 2026

Abstract

Background: Liver fibrosis, the end-stage pathological state of many liver diseases, is primarily driven by the activation of hepatic stellate cells (HSCs) and collagen deposition resulting from various pathogenic causes. Thrombospondin-2 (THBS2), a secreted extracellular matrix glycoprotein encoded by the *TSP gene family*, has been found to activate the TLR4-transforming growth factor-β (TGF-β)/FAK signaling axis and HSCs through autocrine signalling, thereby contributing to the development of liver fibrosis. Latexin (LXN), the only known zinc-dependent metallocarboxypeptidase inhibitor in humans, has not yet been studied for its role in liver fibrosis is yet to be studied. **Methods**: In this study, we used adeno-associated virus 9 (AAV9) to generate a mouse model of liver fibrosis with LXN knockdown and used siLXN to knock down the LXN gene in the human hepatic stellate cell line LX-2. The mechanisms underlying the association between LXN and hepatic fibrosis progression were investigated using quantitative polymerase chain reaction, western blot, immunohistochemistry, and immunofluorescence staining. **Results**: LXN knockdown reduced carbon tetrachloride (CCl_4)-induced liver injury and suppressed activation of hepatic stellate cells, while also inhibiting the expression of α-SMA and collagen I. Furthermore, LXN demonstrates a substantial positive correlation with THBS2, and LXN knockdown was capable of downregulating THBS2. **Conclusion**: The LXN-THBS2 signaling axis may promote liver fibrosis progression by inducing the activation of HSCs.

Keywords: cirrhosis; liver fibrosis; hepatic stellate cells; THBS2; LXN

1. Introduction

Liver fibrosis is the primary pathological process underlying the development of chronic liver disease worldwide, and it is primarily caused by various hepatitis viruses (such as HBV and HCV), metabolic dysfunction-associated steatohepatitis (MASLD, formerly NAFLD), alcoholic liver disease (ALD), and other conditions [1]. This condition is marked by the build-up of a substance called the 'extracellular matrix' (ECM) [2], ultimately leading to cirrhosis, liver failure, and hepatocellular carcinoma (HCC). The primary source of the ECM is a ctivated hepatic stellate cells (HSCs), which play a pivotal role in the development and progression of liver fibrosis [3,4]. Transforming growth factor-β (TGF-β) is a cytokine widely found in multicellular organisms. It can stimulate HSC activation and collagen secretion and has been widely used to induce HSC activation and establish *in vitro* liver fibrosis models [5,6]. Carbon tetrachloride (CCl_4) is an organic compound that can cause inflammation and damage to liver cells. Damaged liver cells release TGF-β, which promotes HSC activation and increases ECM deposition, leading to the progression of liver fibrosis [7]. In this study, a mouse model of liver fibrosis was constructed by intraperitoneal injection of 10% CCl_4 into C57BL/6 mice. Human hepatic stellate cell line (LX-2) cells were treated with TGF-β to activate them, thereby simulating the core pathological process of liver fibrosis.

Latexin (LXN) is the sole endogenous inhibitor of carboxypeptidase A in humans. It is vital for protein turnover and transport, maintaining the number of hematopoietic stem cells, inflammation, and tumors [8,9]. There are reports that LXN is a novel regulator of endothelial cell (EC) morphology maintenance, and LXN knockout can markedly improves vascular permeability, vasodilation, and atherosclerosis in mice [10]. Additionally, LXN is a critical positive modulator of adipocyte differentiation. Mice lacking LXN show resistance to obesity, glucose tolerance, insulin tolerance, and hepatic steatosis induced by high-fat diet (HFD) [7,11]. LXN expression is associated with joint cartilage mineralization during the progression of traumatic osteoarthritis in rats [12]. In a mouse model of DSS-induced colitis, LXN deficiency resulted in more se-

vere colitis. Recent studies have demonstrated that a deficiency in LXN expression is negatively correlated with the prognosis of solid tumors, including prostate cancer, pancreatic cancer, melanoma, thyroid cancer, and HCC, and that it plays a vital role in tumor cell migration and invasion [13–19]. However, there are no relevant studies on its role and mechanism in liver fibrosis.

Thrombospondin-2 (THBS2) is a secreted extracellular matrix glycoprotein encoded by the TSP gene family that plays multiple roles in tissue development, angiogenesis, immune regulation, and disease progression. In NAFLD patients, THBS2 is a useful biomarker for the diagnosis of advanced fibrosis [20]. Zhang *et al.* [21] found that THBS2 can initiate the TLR4-TGF-β/FAK pathway and HSCs, playing a role in the process of liver fibrosis. This study aimed to elucidate the role of the LXN-THBS2 signaling axis in regulating HSC activation, thereby promoting the progression and development of hepatic fibrosis. This is especially evident in the context of the progression and reversal of liver fibrosis. The LXN-THBS2 signalling axis could be a good target for treating liver fibrosis.

2. Materials and Methods

2.1 Patients and Clinical Specimens

As stated in the Ishak scoring system [22], liver tissue samples were collected from four subjects. Patients with liver fibrosis at stages S2, S3, S3/S4, and S4 at the Second People's Hospital of Guangdong Province were included. We strictly adhered to ethical guidelines during the acquisition process to ensure informed consent from the patients. Record clinical information, including patient age, gender, aetiology(including viral hepatitis type, alcohol consumption history, and metabolic syndrome-related indicators, etc.), disease course, liver function indicators (alanine aminotransferase (ALT), aspartate aminotransferase (AST), bilirubin, albumin, and globulin, etc.), imaging examination results (liver stiffness values, ultrasound findings, etc.), and treatment history. All experiments involving human tissue were conducted in accordance with the ethical policies and procedures approved by the Medical Ethics Committee of The Affiliated Guangdong Second Provincial General Hospital of Jinan University. The ethical approval number for this study is 2023-KY-SB-37.

2.2 Mice

24 SPF-grade C57BL/6 J mice, aged 6–8 weeks with a body mass of 19–23 g, were procured from Zhuhai Baishitong Biotechnology Co., Ltd., Guangdong Province, China. A Total of 24 mice were housed in a constant temperature environment (22–23 °C) and were subjected to a standard 12-hour light-dark cycle, with sufficient food and water provided. All animal experiments were conducted in accordance with the ethical guidelines and policies approved by the Laboratory Animal Ethics Committee of The Affiliated Guangdong Second Provincial General Hospital of Jinan University, under approval number 2023-DW-SB-48.

The mice were randomly assigned to four groups with six mice in each group (n = 6): control group (injected with adeno-associated virus 9 (AAV9)-GFP virus), CCl_4-treated model group (injected with AAV9-GFP virus), CCl_4-treated model group (injected with AAV9-LXN shRNA), and control group (injected with AAV9-LXN shRNA). The model group used a CCl_4-induced liver fibrosis model, mixing CCl_4 with olive oil at a ratio of 1:3 to 1:5. The mixture was administered via intraperitoneal injection based on mouse body weight (0.1 mL per 5 g of body weight), the control group received 5 µL/g of corn oil, three times per week for a period of eight weeks.

shRNA sequences targeting LXN were designed and synthesized based on the mouse LXN gene sequence. After annealing to form double strands, the strands were connected to the AAV9 vector. The constructed vector contained promoters, shRNA sequences, and poly(A) tails. This section was constructed to Cyagen Biosciences. The constructed AAV9-LXN shRNA vector and the auxiliary plasmid were co-transfected into HEK293 cells. Following cell culture and virus packaging processes, cell culture supernatants were collected and purified by ultrafiltration and ultracentrifugation to obtain the AAV9-LXN shRNA virus. After determining the virus titer, the virus was stored at –80 °C. Starting from week 3, AAV9-GFP virus and AAV9-LXN shRNA virus (at a dose of 1×10^{11}–1×10^{12} vg/mouse) were injected into the corresponding groups of mice via the tail vein. Following the conclusion of the experimental study, mice were fasted overnight. We administered 50 mg/kg sodium pentobarbital intraperitoneally to anesthetize the mice, measured their body weight, and collected their blood and liver tissue, after which the mice were euthanized by cervical dislocation.

2.3 Blood Biochemistry

The blood collected from mice was centrifuged at 3000 rpm at room temperature for 15 minutes, the supernatant was collected and stored at –80 °C for subsequent experimental analysis. Serum ALT, AST, alkaline phosphatase (ALP), albumin (ALB), total bilirubin (TBIL), total bile acids (TBA), cholesterol (CHO), and triglycerides (TG) levels were measured using an automatic biochemical analyzer (Hitachi 7020, Japan).

2.4 Hepatic Histopathology

After removing the liver tissue, a portion was treated with 4% formaldehyde for 36 hours, then embedded in paraffin and sectioned (4–6 µm thick). The morphology of hepatocytes and the presence of inflammatory cell infiltration were observed using HE staining, and the severity of liver fibrosis was assessed using Sirius red staining.

Table 1. List of primers in PCR amplification.

Gene	Forward primer	Reverse primer
β-Actin	TGTCCACCTTCCAGCAGATGT	AGCTCAGTAACAGTCCGCCTAGA
COL1	GAGGGCCAAGACGAAGACATC	CAGATCACGTCATCGCACAAC
α-SMA	TCGGATACTTCAGCGTCA	GGGAGTAATGGTTGGAATG
LXN	GCGGTTATGTAATGTGGCAG	GTGGTAAGATGAGGTGCTGTAA

COL1, collagen I; α-SMA, alpha-smooth muscle Actin; LXN, latexin.

Table 2. Three sets of LXN-siRNA and NC-siRNA sequences.

Primer name	Sequence (5′-3′)	Length	Tm °C
LXN-siRNA1	CCAGAAGUCAACUUCACAUUUTT	23	50.2
	AAAUGUGAAGUUGACUUCUGGTT	23	50.2
LXN-siRNA2	GAAGUCAACUUCACAUUUGAATT	23	48.4
	UUCAAAUGUGAAGUUGACUUCTT	23	48.4
LXN-siRNA3	CAUCCACAAUACGGCACUAAATT	23	51.9
	UUUAGUGCCGUAUUGUGGAUGTT	23	51.9
NC-siRNA	UUCUCCGAACGUGUCACGUTT	21	52.4
	ACGUGACACGUUCGGAGAATT	21	52.4

2.5 Immunohistochemical Analysis

For immunohistochemical staining of Alpha-Smooth Muscle Actin (α-SMA), collagen I (COL1), and Latexin (LXN), sodium citrate buffer was used to retrieve antigens, and paraffin-embedded sections were subjected to antibody incubation for a duration of 12 hours at 4 °C. Goat anti-rabbit horseradish peroxidase (HRP) secondary antibody (ZK0623, Bioss, China) was then added to each slide and incubated at room temperature for 50 min. The sections were then incubated with 3,3'-Diaminobenzidine (DAB) for two minutes, followed by counterstaining with hematoxylin. Finally, counterstain with blue reagent for ten seconds. The following antibodies were utilized for immunohistochemistry: anti-LXN antibody (1:300, Bioss, bs-1971R), anti-α-SMA antibody (1:250, Bioss, bs-10196R), and anti-COL1 antibody (1:250, Bioss, bs-10423R).

2.6 RNA Extraction and RT-qPCR Analysis

An Animal Tissue Total RNA Extraction Kit (PK10021, Proteintech) was used to extract total RNA from the liver tissue. A spectrophotometer was used to detect the RNA concentration and purity.

The accepted range for the A260/A280 ratio is 1.8–2.0. The reverse transcription process was executed by means of a reverse transcription kit (B639252-0100, Sangon Biotech), and RT-qPCR was conducted using the TB Green® Premix Ex TaqTM II kit (RR420A, TAKARA) on an ABI7500 PCR instrument. We used β-actin as an internal reference gene. The $2^{-\Delta\Delta Ct}$ method was utilized for the statistical analysis. Table 1 presents a list of all the primer sequences.

2.7 Cell Culture and Processing

LX-2 cells were procured from the Shanghai Institute of Cell Biology, Chinese Academy of Sciences. All cell lines used in this study were authenticated by short tandem repeat (STR) profiling and tested negative for mycoplasma contamination. After thawing from liquid nitrogen, the cells were resuspended in DMEM (Gibco, USA) supplemented with 10% fetal bovine serum (Gibco, USA) and 100 U/mL penicillin and streptomycin (Solarbio, Guangzhou, China). Cells were then maintained in a 5% CO_2 incubator for subsequent experiments. The cells were then cultured in six-well plates and grouped as follows: (1) Control group, cultured under standard conditions. (2) TGF-β group: treated with TGF-β1 at 10 ng/mL for 12 hours. (3) TGF-β+ LXN-siRNA group: Following TGF-β1treatment, LXN-siRNA was added and transfected for 24 hours. (4) TGF-β+ siRNA-Ctrl group: Following TGF-β1 treatment, NC-siRNA was added for 24 hours of transfection. LXN-siRNA and a negative control siRNA were designed and synthesized by Shanghai Sangon Biotech Co., Ltd. The sequences are listed in Table 2.

2.8 Immunofluorescence

For liver tissue paraffin sections, fixation with 10% neutral buffered formalin, boil in sodium citrate buffer for 15 minutes, and incubation at room temperature for one hour after blocking with 5% bovine serum albumin (BSA), followed by incubation with the appropriate primary antibody at 37 °C overnight. After thorough washing with PBS, sections were incubated with FITC-labelled goat anti-rabbit IgG at 20 °C for 1 h. Then, the sections were counterstained with 4,6-diamidino-2-phenylindole (DAPI), washed, and mounted using an anti-fluorescence quenching mounting medium (Prolong® Gold). The cells were observed under a

fluorescent microscope (OLYMPUS IX83, Tokyo, Japan). The following antibodies were utilised for immunofluorescence staining: anti-LXN (1:3500; Bioss, bs-1971R) and anti-THBS2 (1:2000; CUSABIO, P35442).

2.9 Protein Extraction and Western Blot Analysis

Total protein was extracted from the liver tissue using a dedicated kit for animal tissues. Lysate proteins from LX-2 cells were prepared using 1:100 PMSF and RIPA buffer, followed by SDS-PAGE to separate 30 micrograms of protein and polyvinylidene difluoride (PVDF) membrane was used to transfer it. For 1 hour at 20 °C, the membrane was blocked with 5% bovine serum albumin (BSA), the primary antibody was incubated with the PVDF membrane at 4 °C overnight, then the PVDF membrane was thoroughly washed with TBST, and incubated with goat anti-rabbit secondary antibody (IgG) (ZK0623) at 20 °C for 70 minutes, followed by ECL chemiluminescence imaging to detect the bands. For the purpose of visual analysis of proteins, ImageJ (NIH, Bethesda, MD, USA) was employed. The primary antibodies utilized for western blotting are listed below: anti-LXN antibody (1:300, Bioss, bs-1971R), anti-α-SMA antibody (1:250, Bioss, bs-10196R), and anti-COL1 antibody (1:250, Bioss, bs-10423R), anti-THBS2 antibody (1:1000, CUSABIO, P35442), and anti-Tubulin antibody (1:2000, Beyotime, AF0001).

2.10 Statistical Analysis

The statistical analyses were conducted using the GraphPad Prism v8.00 software (La Jolla, CA, USA). The experimental data were then compared using Student's *t*-test or analysis of variance. The statistical significance of the results was determined by applying a *p*-value cutoff of 0.05.

3. Results

3.1 LXN is Upregulated in Liver Fibrosis and Regulates Immune Cell Function

We obtained three sets of transcriptome data related to human and mouse liver fibrosis from the GEO database (GSE25583, GSE55747, and GSE84044), from which we screened for differentially expressed genes ($|\text{LogFC}| \geq 1$, $p < 0.005$; $|\text{LogFC}| \geq 2$, $p < 0.00001$; $|\text{LogFC}| \geq 1$, $p < 0.05$). After obtaining the intersection of the three datasets, we identified a common differentially expressed gene LXN (Fig. 1A). Next, LXN expression levels were analyzed in different groups using GEO chips (GSE89377) derived from human cirrhotic tissue samples and GEO chips for mouse cirrhosis (GSE25583 and GSE55747). The results showed that LXN expression was higher in human cirrhosis than in hepatitis, and treatment of mice with CCl_4 to induce cirrhosis also led to increased LXN expression (Fig. 1B–D). Next, we performed differential gene analysis of 124 patients with different stages of liver fibrosis using gene expression profiling chips (GSE84044). Through RNA-seq analysis, we screened for differentially expressed genes (FDR <0.05) at different stages of liver fibrosis. Subsequently, a heat map was generated for the 40 genes with the highest expression levels (Fig. 1E). We performed correlation analysis on the top 20 genes that were upregulated and downregulated in patients with different stages of liver fibrosis, and LXN exhibited a significantly and positively correlated with THBS2 and multiple chemokines (CXCL6, CCL20, CXCL10, CXCL9, CXCL11, and CCL19) (Fig. 1F). THBS2 regulates ECM and collagen deposition, which is linked to liver fibrosis. Pathway and enrichment analyses showed that compared with the low LXN expression group, the high LXN expression group had differentially expressed genes linked to T lymphocyte, granulocyte, and monocyte activation, proliferation, and chemotaxis (Fig. 1G,H).

3.2 The Expression of LXN in Human Liver Tissue Increases With the Progression of Liver Fibrosis

After analyzing the expression profiles of 124 patients with different stages of liver fibrosis (GSE84044), it was established that there was a gradual increase in LXN expression concomitant with the progression of inflammatory activity grading (G0–G4) and fibrosis staging (S0–S4) (Fig. 2A,B). To validate this result, we collected liver tissue samples from four patients with liver fibrosis stages S2, S3, S3/S4, and S4, and performed HE staining, Sirius red staining, and LXN immunohistochemical staining. HE staining revealed that as the stage of liver fibrosis increased, the portal areas gradually expanded, forming fibrous septa, and the hepatic lobule structure became disordered with increased inflammatory cell infiltration. Sirius Red staining showed that collagen deposition gradually increased and fibrous septa formed as liver fibrosis progressed. The immunohistochemical staining results for LXN were consistent with our expectations, with LXN expression increasing as the stage of liver fibrosis progressed (Fig. 2C, **Supplementary Fig. 1A,B**).

3.3 Weight and Blood Biochemical Index Measurements of Four Groups of Mice

This study used a CCl_4-induced liver fibrosis model in which mice received intraperitoneal injections of CCl_4 for eight weeks. To determine whether LXN knockout could alleviate CCl_4-induced liver fibrosis in mice, AAV9-LXN-shRNA or control (GFP) was injected into C57BL/6 mice starting at week 3 (Fig. 3A). After the experiment, the mice were euthanised and whole blood and liver tissue were collected. The body weight and ALT, AST, ALP, ALB, TBIL, TBA, CHO, and TG levels of the mice were measured (Fig. 3B–J). The results showed that murine subjects in the CCl_4-modelling group exhibited a reduced mean body mass compared with the control group, and indicators such as TBIL, TBA, ALT, AST and ALP were all elevated, indicating that CCl_4 treatment damaged the liver function

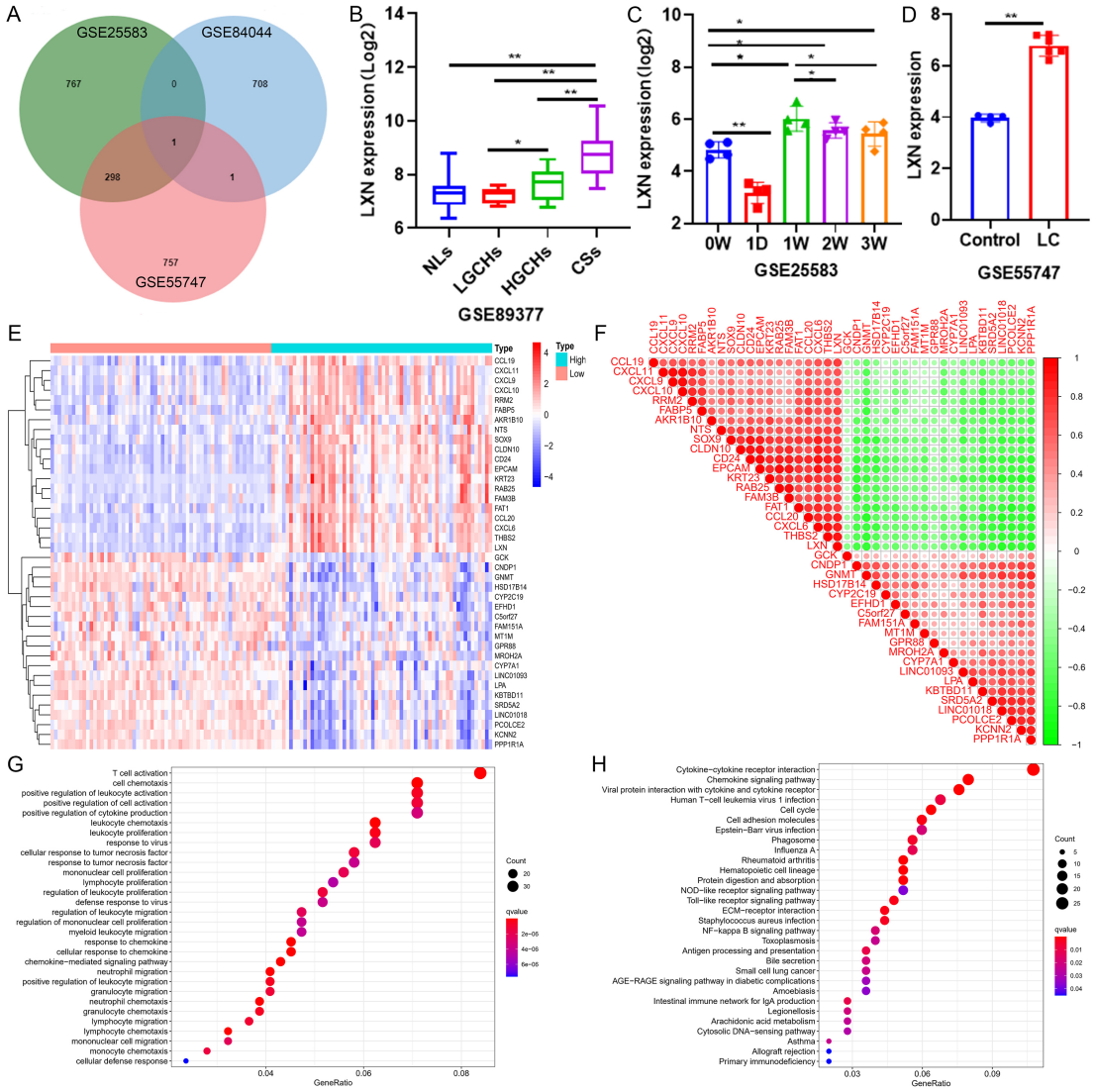

Fig. 1. Latexin (LXN) is upregulated in liver fibrosis and highly correlated with Thrombospondin-2 (THBS2). (A) The Venn diagram illustrates the correlations among differentially expressed genes across three liver fibrosis datasets. (B) LXN expression in four distinct pathological states within the human liver tissue dataset. NLs, Normal liver tissue; LGCHs, Low-grade chronic hepatitis; HGCHs, High-grade chronic hepatitis; CSs, Cirrhosis. * $p < 0.05$, ** $p < 0.01$. (C) Expression of LXN in mouse liver fibrosis datasets following no carbon tetrachloride (CCl_4) treatment, and at different time points following CCl_4 treatment. * $p < 0.05$, ** $p < 0.01$. (D) Expression of LXN in healthy individuals and patients with liver cirrhosis. ** $p < 0.01$. (E) The heatmap depicts the differential expression patterns of the top 40 most highly expressed genes across 124 patients at different stages of liver fibrosis. (F) The correlation heatmap illustrates the associations between the top 20 genes showing upregulation and downregulation. (G,H) Pathway and enrichment analysis of the high-expression LXN group.

of mice. Following LXN knockdown using AAV9-LXN-shRNA, the levels of TBIL, TBA, ALT, AST, and ALP were reduced compared to the model group. TBA is a sensitive marker of liver damage and can directly participate in the fibrotic process through mechanisms such as HSC activation and oxidative stress. This finding suggests that suppression of LXN may lead to a reduction in HSC activation and oxidative stress, consequently alleviating CCl_4-induced liver injury and mitigating liver fibrosis.

3.4 AAV9-LXN shRNA Reverses CCl_4-Induced Liver Fibrosis

Subsequently, the present study investigated the potential of AAV9-LXN shRNA to reduce liver fibrosis and protect the liver from the harmful effects of CCl_4. Photographs of the isolated livers were taken, and HE and Sirius red staining were utilised in order to ascertain the histopathological status of the mouse liver tissue and collagen deposition. Immunohistochemical staining for α-SMA, collagen I, and LXN was performed to examine HSC acti-

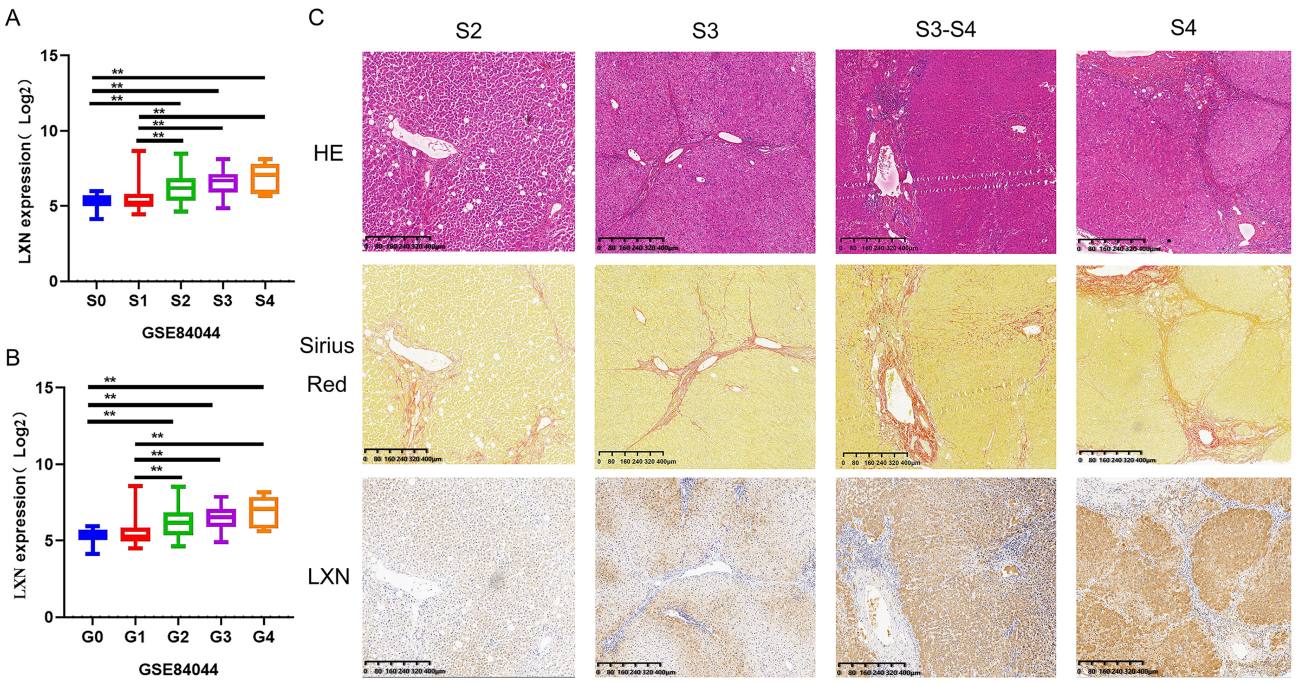

Fig. 2. Expression of LXN in human liver tissue increases with the progression of liver fibrosis. All experiments were performed in triplicate (n = 3). (A,B) In a dataset comprising 124 patients with distinct stages of hepatic fibrosis, the expression of LXN correlates with both the grading and staging of fibrosis. ** $p < 0.01$. (C) Histological, Sirius red, and immunohistochemical staining findings in four patients with different stages of liver fibrosis. Scale is 400 µm.

vation and LXN expression. As shown in Fig. 4A, a significant decrease in liver volume was observed in mice exposed to CCl_4 in compared to the control group. HE staining revealed a disordered hepatic lobule structure, dilated sinusoids, inflammatory cell infiltration, and interlobular septum formation. Sirius red staining showed a significant increase in collagen fiber deposition, whereas the liver tissue in the reversal group spontaneously recovered. These results demonstrated the successful establishment of a liver fibrosis model. Immunohistochemical staining results showed that CCl_4-induced HSCs were activated, with a substantial increase in the number of α-SMA+ cells in the liver; collagen I also showed a similar trend. However, treatment with AAV9-LXN shRNA alleviated these changes. As HSCs are activated in the liver, LXN expression was significantly upregulated. We also performed quantitative analysis of Sirius Red staining and immunohistochemical staining, as shown in **Supplementary Fig. 1C,D**. We subsequently performed immunofluorescence staining for THBS2, and the results were consistent with the changes observed in LXN. THBS2 expression was upregulated in the CCl_4-induced liver fibrosis model group, and LXN interference led to its downregulation (Fig. 4B).

Additionally, RT-qPCR and Western blot analyses further confirmed these results, showing that the CCl_4-treated groups exhibited significantly increased LXN expression and markedly elevated HSC activation indices, whereas LXN-silenced mice in the reversal group demonstrated reduced HSC activation indices. Furthermore, the expression of these genes was significantly reduced following LXN knockdown (**Supplementary Fig. 2** and Fig. 4C,D). In summary, liver fibrosis upregulates LXN expression, and LXN knockdown can reverse and regress liver fibrosis.

3.5 siLXN Interference can Weaken the Activation of HSCs

The LX-2 cells were subjected to a treatment with TGF-β to induce their activation, and LXN-siRNA was used to silence LXN in TGF-β-treated LX-2 cells. The duration of the treatment was 10 h. After treatment, Oil red O staining and immunofluorescence analyses of LXN and THBS2 were performed. The proteins were extracted for Western blot analysis. Unactivated LX-2 cells and empty siRNA were used as controls. Immunofluorescence staining showed that after TGF-β induction, the fluorescence intensity of LXN increased, whereas that in the LXN-siRNA group was significantly reduced, indicating that the cell model was successfully established. The results of THBS2 immunofluorescence staining were consistent with those of LXN, with TGF-β induction increasing the fluorescence intensity, whereas knockdown of LXN reduced the expression of THBS2 (Fig. 5A). Oil red staining results showed that LX-2 cells treated with TGF-β had larger volumes than unactivated cells, with a flat, star-shaped, or polygonal morphology, dense cell arrangement, darker nuclear staining, and a marked reduction in lipid droplets. Treatment with LXN-siRNA reversed these effects (Fig. 5B). Western blot

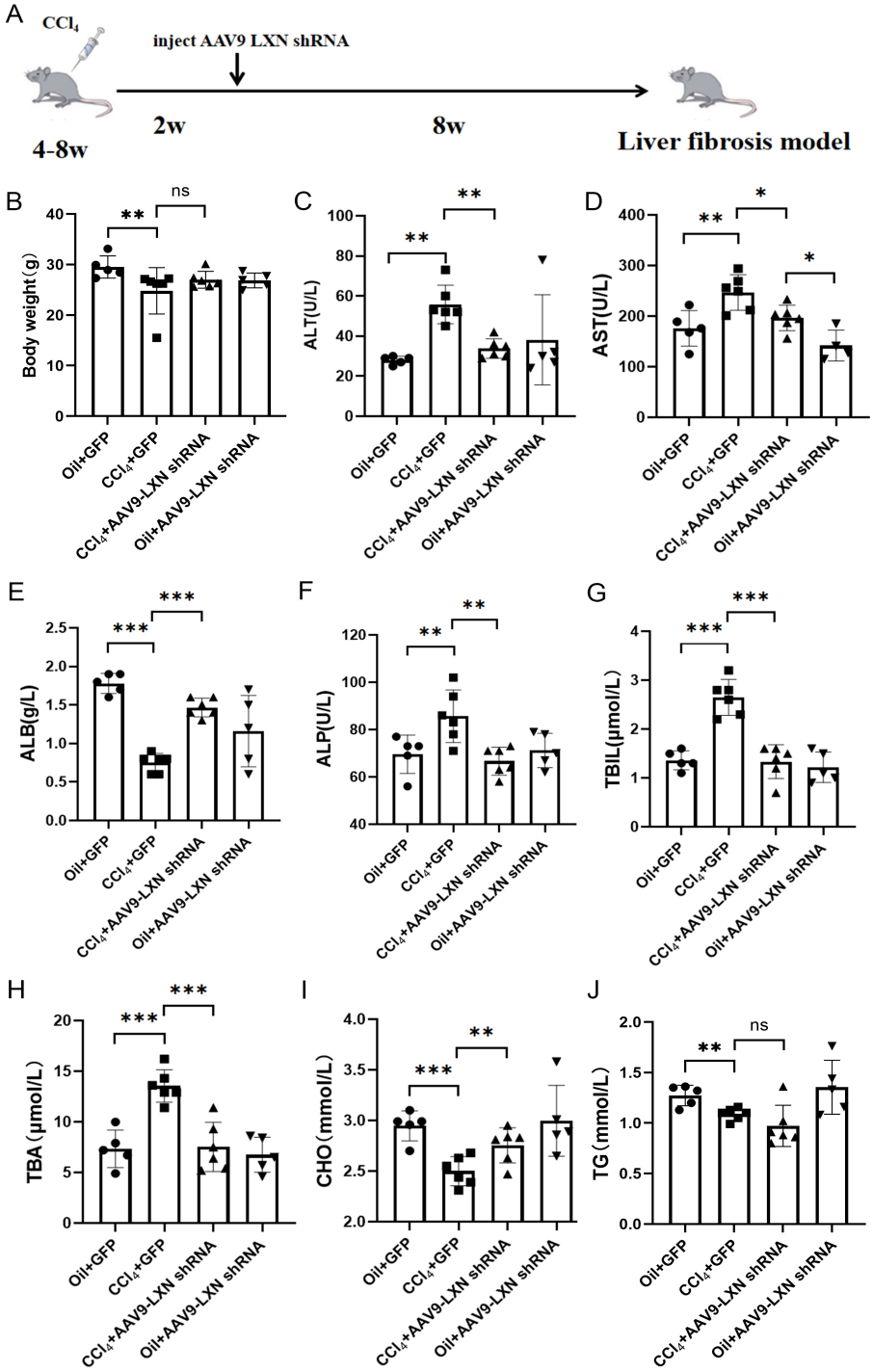

Fig. 3. Weight and blood biochemical parameters in the four groups of mice. (A) Schematic diagram of the treatment protocol for the CCl_4-induced adeno-associated virus 9 (AAV9)-LXN-shRNA mouse model. (B–J) Body weight and Serum Alanine Aminotransferase (ALT), Aspartate Aminotransferase (AST), alkaline phosphatase (ALP), albumin (ALB), total bilirubin (TBIL), total bile acids (TBA), cholesterol (CHO), and triglycerides (TG) levels in the four mouse groups. * $p < 0.05$, ** $p < 0.01$, *** $p < 0.001$, ns indicates no significant difference.

results confirmed that, compared with untreated cells, TGF-β induction can lead to HSC activation and upregulation of collagen I and α-SMA expression, while LXN silencing can weaken LX-2 cell activation and downregulate collagen I and α-SMA expression. However, the empty siRNA vector group did not show this change. THBS2 expression showed a trend consistent with that of LXN (Fig. 5C,D).

Single-cell sequencing data of liver tissues during hepatic fibrosis, retrieved from the GEO database (GSE174748), was further analyzed. Unsupervised cluster-

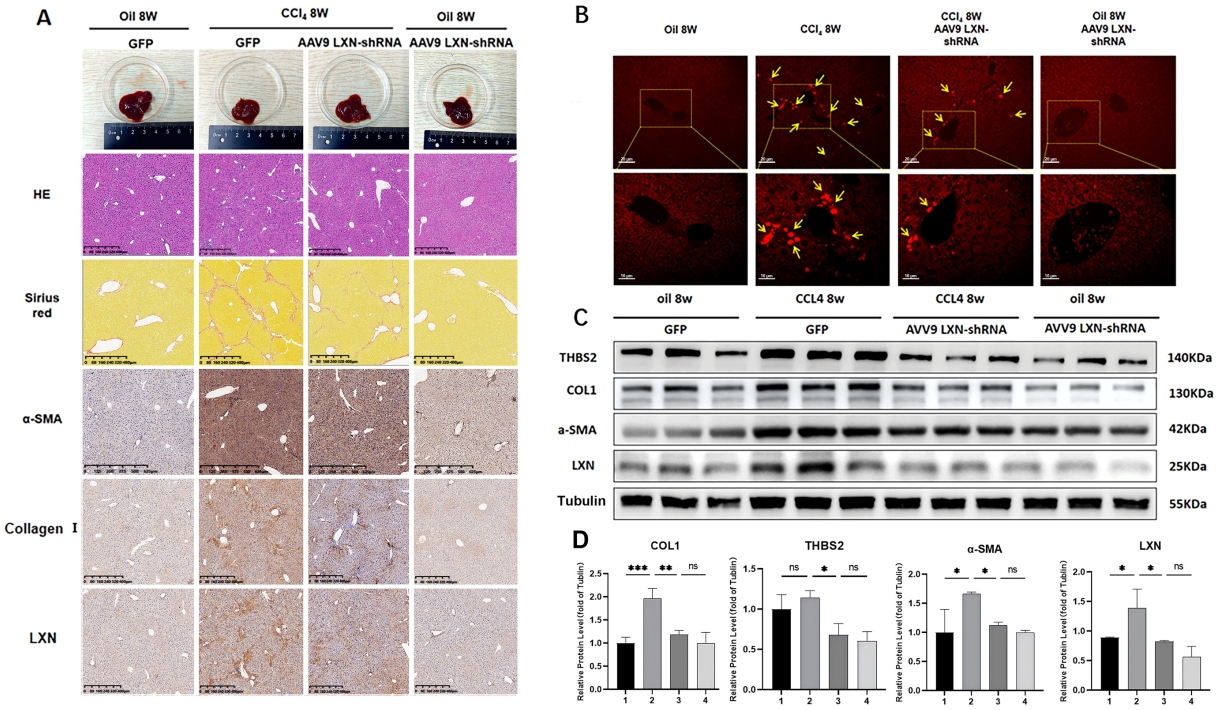

Fig. 4. AAV9-LXN shRNA reverses CCl_4-induced liver fibrosis. All experiments were performed in triplicate (n = 3). (A) Histological examination of liver tissue from oil 8w, CCl_4 8w-induced model, CCl_4 8w AAV9 LXN-shRNA, and oil 8w AAV9 LXN-shRNA-treated mice via hematoxylin and eosin staining, Sirius red staining, and immunohistochemical staining for α-SMA, collagen I (COL1), and LXN. Scale bars are as indicated. The scale of HE staining and Sirius red staining is 400 µm, The immunohistochemical staining scale of α-SMA is 625 µm, Collagen I and LXN is 400 µm. (B) Immunofluorescence staining of THBS2 in liver tissue from four groups of mice, the area indicated by the arrow is the positive zone, the original image and enlarged graphic are at magnifications of 20× (20 µm) and 40× (10 µm) respectively. (C) Western blotting and quantitative analysis of LXN, THBS2, α-SMA, and COL1 proteins in liver tissue from four groups of mice, using tubulin as the internal reference protein. (D) Quantitative analysis by Western blot, oil 8w, CCl_4 8w-induced model, CCl_4 8w AAV9 LXN-shRNA, and oil 8w AAV9 LXN-shRNA are denoted as 1/2/3/4 respectively. * $p < 0.05$, ** $p < 0.01$, *** $p < 0.001$, ns indicates no significant difference.

ing of the qualified single-cell dataset identified 10 distinct cell clusters (**Supplementary Fig. 3A**). Subsequently, a panel of classical HSC marker genes (DCN, HGF, ACTA2, and ADAMTSL2) was utilized to validate and annotate each cell cluster (**Supplementary Fig. 3B**). Via this marker gene-mediated identification strategy, the HSC cluster was successfully localized and defined within the heterogeneous cellular population of liver tissues (**Supplementary Fig. 3C**). Further differential expression analysis demonstrated that the LXN gene was specifically highly expressed in HSCs, with negligible expression detected in other cell clusters (**Supplementary Fig. 3D**).

4. Discussion

Excessive ECM deposition and HSC activation in liver tissue are significant factors in fibrosis and profibrotic cytokine formation [23,24]. Liver fibrosis is reversible, unlike other serious liver conditions such as cirrhosis and HCC. Liver fibrosis can be reversed or eliminated by inhibiting HSC activation through certain pathways [25].

Using the Gene Expression Omnibus (GEO) database, we found that LXN is upregulated in advanced liver fibrosis, with increased expression as the stage progresses, and increased LXN expression in primary HSCs, suggesting that it is closely related to liver fibrosis. Current research indicates that LXN plays a role in protein turnover, maintaining hematopoietic stem cell numbers, inflammation, and tumorigenesis. However, its role and underlying mechanisms in liver fibrosis remain unclear. CCl_4-induced liver fibrosis in animals is widely used to simulate the pathogenesis of liver fibrosis in humans [26]. CCl_4 induces liver fibrosis in C57BL/6 mice. AAV9-LXN shRNA was used for LXN knockdown. By measuring the levels of liver injury markers, such as ALT, AST, and TBA, we found that LXN knockdown reduced CCl_4-induced liver injury. Additionally, the results demonstrated inhibition of α-SMA and collagen I mRNA and protein expression, thereby reversing CCl_4-induced liver fibrosis. Cell experiments have confirmed that LXN siRNA can inhibit the activation of HSCs and suppress the secretion of α-SMA and collagen I. α-SMA and COL1 are core molecular markers

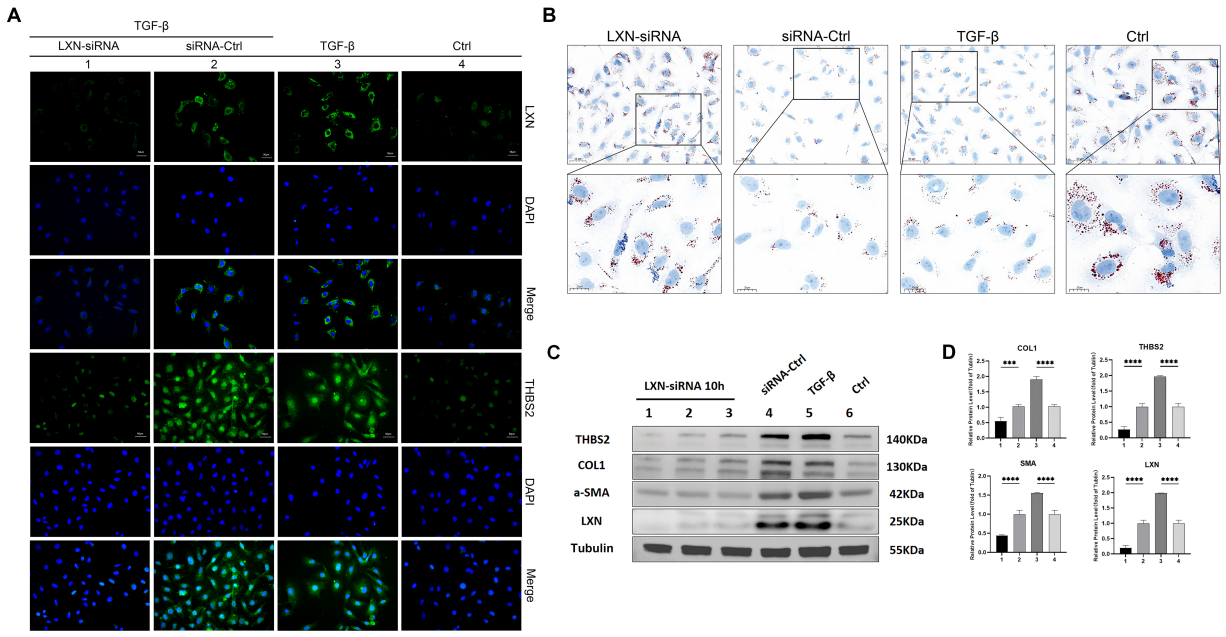

Fig. 5. LXN siRNA interference reduces the activation of hepatic stellate cells (HSCs). All experiments were performed in triplicate (n = 3). (A) Immunofluorescence staining for LXN and THBS2 in cells from the control group, transforming growth factor-β (TGF-β)-induced activation group, TGF-β-siLXN knockdown group, and TGF-β-siRNA control group. Scale bars are 50 µm. (B) Oil red staining of the above four cell groups. Scale bars are 50 µm and 25 µm. (C,D) Western blot analysis and quantitative assessment of four cellular proteins—LXN, THBS2, COL1, and α-SMA—were conducted, with Tubulin employed as the internal control protein. LXN-siRNA, siRNA-Ctrl, TGF-β and Ctrl are denoted as 1/2/3/4 respectively (D). *** $p < 0.001$, **** $p < 0.0001$.

in the pathological progression of liver fibrosis, representing HSC activation and abnormal deposition of ECM, respectively. α-SMA is a marker of activated HSCs. During liver fibrosis, quiescent HSCs transform into activated myofibroblasts, which express α-SMA [27]. COL1 is a significant constituent of the extracellular matrix and is excessively deposited during liver fibrosis. In normal liver tissue, the extracellular matrix is primarily composed of type IV collagen and laminin; however, during fibrosis, type I collagen becomes the predominant component. Studies have shown that as fibrosis progresses, COL1 expression gradually increases [28,29]. These data suggest that LXN may induces liver fibrosis by activating HSCs.

At the same time, analysis of the GEO database revealed a positive correlation between LXN and THBS2. Previous studies have reported that LXN regulates THBS1 to form a signaling cascade that plays a pivotal role in regulating the function of hematopoietic stem cells, stress responses, and cancer development under steady-state conditions [30,31]. THBS2 has been shown to activate the TLR4-TGF-β/FAK signaling axis and HSCs, playing a crucial role in the development of liver fibrosis. The results of this study showed that THBS2 expression was upregulated in liver fibrosis models and primary cultured HSCs, whereas LXN knockdown downregulated THBS2 expression. Since both THBS2 and THBS1 are members of the thrombin-responsive protein family, we hypothesized that the LXN-THBS2 axis regulates the development of liver fibrosis by activating HSCs.

Nevertheless, this study had some limitations. For example, it is unclear how LXN regulates THBS2 expression. Research has identified that LXN regulates THBS1 transcription through the Rps3-NF-κB pathway [8]. LXN has been demonstrated to bind to Rps3, thereby impeding its entry into the nucleus. In the absence of LXN, Rps3 is able to enter the nucleus unimpeded, activate the NF-κB pathway, and inhibit THBS1 transcription. Sustained activation of inflammatory signaling is pivotal for the progression of liver fibrosis. The NF-κB pathway, a pivotal regulator of inflammatory responses, may be implicated in the upregulation of THBS2 upon its activation; however, the precise molecular mechanisms require further experimental validation.

Moreover, only knockdown experiments were conducted for LXN, omitting the need for overexpression experiments. Further studies are needed to determine how increased LXN expression causes liver fibrosis. Further investigation is necessary to elucidate the mechanism by which THBS2 activates HSCs and to determine whether other signaling pathways are involved in this process.

5. Conclusion

In summary, this study demonstrates that knocking out LXN downregulates THBS2 expression and reverses CCl_4-induced mouse liver fibrosis and TGF-β-induced LX-2 cell

fibrosis by reducing hepatic stellate cell activation. The LXN-THBS2 axis may contribute to the development of liver fibrosis by activating HSCs.

Availability of Data and Materials

The datasets used or analyzed during the current study are available from the corresponding author on reasonable request.

Author Contributions

HYW, HYJ, and YCY devised the research plan; DLC provided academic guidance and technical support for this research. HYJ, SYW conducted data analysis, HYW, HYJ, SYW, XRL and XT conducted experimental research, XT, YCY, DLC provided advice for the research, and HYW authored the manuscript. All authors contributed to editorial changes in the manuscript. All authors read and approved the final manuscript. All authors have participated sufficiently in the work and agreed to be accountable for all aspects of the work.

Ethics Approval and Consent to Participate

This study has been approved by the Institutional Review Board (IRB) of The Affiliated Guangdong Second Provincial General Hospital of Jinan University, approval number [2023-KY-SB-37]. All participants were provided with information regarding the study and gave their written informed consent prior to participation. This study was conducted in compliance with the Declaration of Helsinki and all applicable ethical guidelines. The animal study protocol was approved by the Animal Care and Use Committee (ACUC) of The Affiliated Guangdong Second Provincial General Hospital of Jinan University, protocol number [2023-DW-SB-48]. The study adhered to the guidelines set by the committee.

Acknowledgment

Not applicable.

Funding

This research received no external funding.

Conflict of Interest

The authors declare no conflict of interest.

Supplementary Material

Supplementary material associated with this article can be found, in the online version, at https://doi.org/10.31083/FBL46251.

References

[1] Gressner AM, Weiskirchen R. Modern pathogenetic concepts of liver fibrosis suggest stellate cells and TGF-beta as major players and therapeutic targets. Journal of Cellular and Molecular Medicine. 2006; 10: 76–99. https://doi.org/10.1111/j.1582-4934.2006.tb00292.x.

[2] Cordero-Espinoza L, Huch M. The balancing act of the liver: tissue regeneration versus fibrosis. The Journal of Clinical Investigation. 2018; 128: 85–96. https://doi.org/10.1172/JCI93562.

[3] Toosi AEK. Liver Fibrosis: Causes and Methods of Assessment, A Review. Romanian Journal of Internal Medicine = Revue Roumaine De Medecine Interne. 2015; 53: 304–314. https://doi.org/10.1515/rjim-2015-0039.

[4] Wang X, Wang Y, Yang M, Zhao T, Feng Z, Zhou Y, *et al*. Single-cell Transcriptome Analysis Reveals the Potential Role of Hepatic Stellate Cells in Liver Fibrosis. Frontiers in Bioscience (Landmark Edition). 2025; 30: 42394. https://doi.org/10.31083/FBL42394.

[5] Gressner AM, Weiskirchen R, Breitkopf K, Dooley S. Roles of TGF-beta in hepatic fibrosis. Frontiers in Bioscience: a Journal and Virtual Library. 2002; 7: d793–d807. https://doi.org/10.2741/A812.

[6] Dewidar B, Meyer C, Dooley S, Meindl-Beinker AN. TGF-β in Hepatic Stellate Cell Activation and Liver Fibrogenesis-Updated 2019. Cells. 2019; 8: 1419. https://doi.org/10.3390/cells8111419.

[7] Friedman SL. Mechanisms of hepatic fibrogenesis. Gastroenterology. 2008; 134: 1655–1669. https://doi.org/10.1053/j.gastro.2008.03.003.

[8] Zhang C, Liang Y. Latexin and hematopoiesis. Current Opinion in Hematology. 2018; 25: 266–272. https://doi.org/10.1097/MOH.0000000000000428.

[9] Zhang C, Fondufe-Mittendorf YN, Wang C, Chen J, Cheng Q, Zhou D, *et al*. Latexin regulation by HMGB2 is required for hematopoietic stem cell maintenance. Haematologica. 2020; 105: 573–584. https://doi.org/10.3324/haematol.2018.207092.

[10] He G, Kan S, Xu S, Sun X, Li R, Shu W, *et al*. LXN deficiency regulates cytoskeleton remodelling by promoting proteolytic cleavage of Filamin A in vascular endothelial cells. Journal of Cellular and Molecular Medicine. 2021; 25: 6815–6827. https://doi.org/10.1111/jcmm.16685.

[11] Kan S, Li R, Tan Y, Yang F, Xu S, Wang L, *et al*. Latexin deficiency attenuates adipocyte differentiation and protects mice against obesity and metabolic disorders induced by high-fat diet. Cell Death & Disease. 2022; 13: 175. https://doi.org/10.1038/s41419-022-04636-9.

[12] Martínez-Calleja A, Cruz R, Miranda-Sánchez M, Fragoso-Soriano R, Vega-López MA, Kouri JB. Latexin expression correlated with mineralization of articular cartilage during progression of post-traumatic osteoarthritis in a rat model. Histology and Histopathology. 2020; 35: 269–278. https://doi.org/10.14670/HH-18-151.

[13] Zhang M, Osisami M, Dai J, Keller JM, Escara-Wilke J, Mizokami A, *et al*. Bone Microenvironment Changes in Latexin Expression Promote Chemoresistance. Molecular Cancer Research: MCR. 2017; 15: 457–466. https://doi.org/10.1158/1541-7786.MCR-16-0392.

[14] Xue ZX, Zheng JH, Zheng ZQ, Cai JL, Ye XH, Wang C, *et al*. Latexin inhibits the proliferation of CD133+ miapaca-2 pancreatic cancer stem-like cells. World Journal of Surgical Oncology. 2014; 12: 404. https://doi.org/10.1186/1477-7819-12-404.

[15] Oldridge EE, Walker HF, Stower MJ, Simms MS, Mann VM, Collins AT, *et al*. Retinoic acid represses invasion and stem cell phenotype by induction of the metastasis suppressors RARRES1 and LXN. Oncogenesis. 2013; 2: e45. https://doi.org/10.1038/oncsis.2013.6.

[16] Xue Z, Zhou Y, Wang C, Zheng J, Zhang P, Zhou L, *et al*. Latexin exhibits tumor-suppressor potential in pancreatic ductal adenocarcinoma. Oncology Reports. 2016; 35: 50–58. https://doi.org/10.3892/or.2015.4353.

[17] Seed RI, Taurozzi AJ, Wilcock DJ, Nappo G, Erb HHH, Read ML, *et al*. The putative tumour suppressor protein Latexin is secreted by prostate luminal cells and is downregulated in malignancy. Scientific Reports. 2019; 9: 5120. https://doi.org/10.1038/s41598-019-41379-8.

[18] Muthusamy V, Premi S, Soper C, Platt J, Bosenberg M. The hematopoietic stem cell regulatory gene latexin has tumor-suppressive properties in malignant melanoma. The Journal of Investigative Dermatology. 2013; 133: 1827–1833. https://doi.org/10.1038/jid.2013.48.

[19] Ni QF, Tian Y, Kong LL, Lu YT, Ding WZ, Kong LB. Latexin exhibits tumor suppressor potential in hepatocellular carcinoma. Oncology Reports. 2014; 31: 1364–1372. https://doi.org/10.3892/or.2014.2966.

[20] Kozumi K, Kodama T, Murai H, Sakane S, Govaere O, Cockell S, *et al*. Transcriptomics Identify Thrombospondin-2 as a Biomarker for NASH and Advanced Liver Fibrosis. Hepatology (Baltimore, Md.). 2021; 74: 2452–2466. https://doi.org/10.1002/hep.31995.

[21] Zhang N, Wu X, Zhang W, Sun Y, Yan X, Xu A, *et al*. Targeting thrombospondin-2 retards liver fibrosis by inhibiting TLR4-FAK/TGF-β signaling. JHEP Reports: Innovation in Hepatology. 2024; 6: 101014. https://doi.org/10.1016/j.jhepr.2024.101014.

[22] Ishak K, Baptista A, Bianchi L, Callea F, De Groote J, Gudat F, *et al*. Histological grading and staging of chronic hepatitis. Journal of Hepatology. 1995; 22: 696–699. https://doi.org/10.1016/0168-8278(95)80226-6.

[23] Lin CY, Adhikary P, Cheng K. Cellular protein markers, therapeutics, and drug delivery strategies in the treatment of diabetes-associated liver fibrosis. Advanced Drug Delivery Reviews. 2021; 174: 127–139. https://doi.org/10.1016/j.addr.2021.04.008.

[24] Sun M, Kisseleva T. Reversibility of liver fibrosis. Clinics and Research in Hepatology and Gastroenterology. 2015; 39 Suppl 1: S60–S63. https://doi.org/10.1016/j.clinre.2015.06.015.

[25] Zong Z, Liu J, Wang N, Yang C, Wang Q, Zhang W, *et al*. Nicotinamide mononucleotide inhibits hepatic stellate cell activation to prevent liver fibrosis via promoting PGE_2 degradation. Free Radical Biology & Medicine. 2021; 162: 571–581. https://doi.org/10.1016/j.freeradbiomed.2020.11.014.

[26] Forbes SJ, Newsome PN. Liver regeneration - mechanisms and models to clinical application. Nature Reviews. Gastroenterology & Hepatology. 2016; 13: 473–485. https://doi.org/10.1038/nrgastro.2016.97.

[27] Friedman SL. Hepatic stellate cells: protean, multifunctional, and enigmatic cells of the liver. Physiological Reviews. 2008; 88: 125–172. https://doi.org/10.1152/physrev.00013.2007.

[28] Kisseleva T, Brenner DA. Hepatic stellate cells and the reversal of fibrosis. Journal of Gastroenterology and Hepatology. 2006; 21 Suppl 3: S84–S87. https://doi.org/10.1111/j.1440-1746.2006.04584.x.

[29] Inagaki Y, Okazaki I. Emerging insights into Transforming growth factor beta Smad signal in hepatic fibrogenesis. Gut. 2007; 56: 284–292. https://doi.org/10.1136/gut.2005.088690.

[30] Kopp HG, Hooper AT, Broekman MJ, Avecilla ST, Petit I, Luo M, *et al*. Thrombospondins deployed by thrombopoietic cells determine angiogenic switch and extent of revascularization. The Journal of Clinical Investigation. 2006; 116: 3277–3291. https://doi.org/10.1172/JCI29314.

[31] Li Q, Ahuja N, Burger PC, Issa JP. Methylation and silencing of the Thrombospondin-1 promoter in human cancer. Oncogene. 1999; 18: 3284–3289. https://doi.org/10.1038/sj.onc.1202663.